Original Article

Hydrolytic degradation of star-shaped poly(ε-caprolactone)s with different number of arms and their cytotoxic effects

Marijana Ponjavic[1] (iD)**, Marija S Nikolic[1]** (iD)**,
Sanja Stevanovic[2], Jasmina Nikodinovic-Runic[3],
Sanja Jeremic[3], Aleksandar Pavic[3]
and Jasna Djonlagic[1]**

Abstract

Star-shaped polymers of biodegradable aliphatic polyester, poly(ε-caprolactone), PCL, with different number of arms (three, four, and six) were synthesized by ring-opening polymerization initiated by multifunctional alcohols used as cores. As potential biomaterials, synthesized star-shaped poly(ε-caprolactone)s, sPCL, were thoroughly characterized in terms of their degradation under different pH conditions and in respect to their cytotoxicity. The in vitro degradation was performed in phosphate buffer (pH 7.4) and hydrochloric acid solution (pH 1.0) over 5 weeks. Degradation of sPCL films was followed by the weight loss measurements, GPC, FTIR, and AFM analysis. While the most of the samples were stable against the abiotic hydrolysis at pH 7.4 after 5 weeks of degradation, degradation was significantly accelerated in the acidic medium. Degradation rate of polymer films was affected by the polymer architecture and molecular weight. The molecular weight profiles during the degradation revealed random chain scission of the ester bonds indicating bulk degradation mechanism of hydrolysis at pH 7.4, while acidic hydrolysis proceeded through the bulk degradation associated with surface erosion, confirmed by AFM. The in vitro toxicity tests, cytotoxicity applying normal human fibroblasts (MRC5) and embryotoxicity assessment (using zebra fish model, *Danio rerio*), suggested those polymeric materials as suitable for biomedical application.

[1]Faculty of Technology and Metallurgy, University of Belgrade, Belgrade, Serbia
[2]Institute of Chemistry, Technology and Metallurgy, University of Belgrade, Belgrade, Serbia
[3]Institute of Molecular Genetics and Genetic Engineering, University of Belgrade, Belgrade, Serbia

Corresponding author:
Marijana Ponjavic, Faculty of Technology and Metallurgy, University of Belgrade, Karnegijeva 4, Belgrade 11000, Serbia.
Email: mponjavic@tmf.bg.ac.rs

Graphical abstract
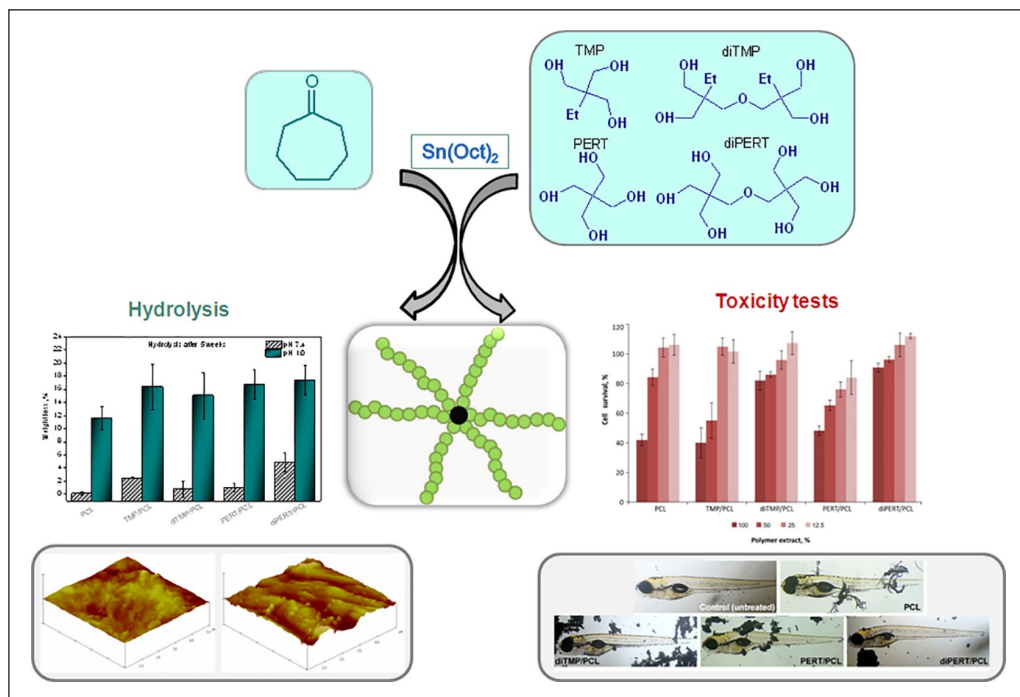
Introduction

The accumulation of polymer waste and the impact of polymeric materials on the environment over past years have put the biodegradable aliphatic polyesters in the research focus as a promising material to replace conventional plastics. Biodegradable polyesters have great potential in suppression of environmental pollution, but also have been widely used in various biomedical fields.[1] Recently, branched polymers have emerged as a new type of biomaterials due to their high performance in sustained, controlled, and targeted delivery of therapeutic and diagnostic agents, as well as in tissue engineering.[2] Among them, star-shaped polyesters which consist of at least three linear polymeric chains (arms) with radial arrangement around a central molecular fragment (core) appear to be the most promising owning to their smaller hydrodynamic volume, internal and peripheral functionality, lower melt and solution viscosities compared to their linear one.[3–5]

The poly(ε-caprolactone), PCL, an aliphatic polyester, is a semi-crystalline, hydrophobic, and biodegradable polymer.[6] PCL is synthetic biomaterial of choice in controlled drug delivery systems due to its biocompatibility, good permeability to many kinds of drugs and non-toxicity.[7,8] In contrast, relatively high hydrophobicity and crystallinity of PCL are responsible for its quite slow degradation which further could remarkably limit its use as biomaterial. One of the ways to improve PCL biodegradability is to introduce hydrophilic, soft segments into PCL chains, that is, poly(ethylene oxide) which was the objective of our previous works.[9,10] Another approach is to decrease crystallinity by synthesizing star-shaped PCL because branched structure has more free chain ends which disrupt well-ordered crystal structure of linear PCL.[11] Moreover, star-shaped PCLs with well-defined structure have great potential in multiple fields of chemistry, biochemistry, engineering due to the higher molecular weight and functionality per unit volume that set them apart from linear PCL.[12–15]

In the previous studies, various multi-functional alcohols were used to initiate the ring-opening polymerization (ROP) of ε-caprolactone where the number of hydroxyl functionalities dictates the final number of arms. The most used multifunctional cores to produce three, four, and six armed star polymers were trimethylolpropane (TMP), ditrimethylolpropane (diTMP), pentaerythritol (PERT), dipentaerythritol (diPERT), but a comprehensive list of star PCLs includes also glycerol, erythritol, sorbitol, xylitol, etc.[11,16–18] The multi-armed structure was found to have great impact on the thermal properties and crystallization and some studies reported that the melting temperature (T_m) and degree of crystallinity (X_c) are affected by both the molecular weight and number of arms.[19] The molecular weight and multi-armed structure also played an important role in thermal stability of sPCL, which is important from the thermal processing aspect.[20] Further, star-shaped PCL exhibit great ability to be modified through end-functionalization and conversion of hydroxyl end group to block copolymers which can easily form self-assembled micelles suitable as drug delivery systems thus improving drug loading, efficiency of encapsulation, and release in sustained manner.[16,21]

Hydrolytic degradation of PCL and PCL based polymers has been intensively investigated and the great effort has been made to explain the mechanism through which the degradation occurs. Degradation patterns of linear PCL, PCL block copolymers, and PCL networks have been studied under the different degradation conditions: different pH, under physiological conditions, non-catalyzed, and catalyzed by enzymes.[22–24] The degradation of PCL based polymers is long-term process that could be remarkably enhanced in the presence of enzymes, but accelerated degradation could also be achieved in acidic or basic medium. Although a lot of research was conducted on the synthesis, characterization, and potential application of PCL with star-shaped architecture,[25–27] hydrolytic degradation and the effect of pH of degradation medium on degradation rate have not been highlighted sufficiently. Also, not enough attention was paid on cytotoxic effects of star-shaped PCL with different architecture which is important for their final application. Therefore, in this work we synthesized a series of star-shaped PCL with well-defined structure that is, number of arms (three, four, and six) and similar length of arms (5000 g/mol). Multifunctional alcohols, such as trimethylolpropane (TMP), pentaerythritol (PERT), ditrimethylolpropane (diTMP), and dipentaerythritol (diPERT) were used as initiators in ring-opening polymerization of ε-caprolactone. The length of PCL arms was controlled by the molar ratio of monomer to initiating hydroxyl group [CL]/[OH]=44. Although this type of star-shaped PCL based polyesters, with TMP, diTMP, PERT, and diPERT as multifunctional initiators, have been frequently investigated in terms of structural, thermal, and crystallization properties, to the best of our knowledge, there are no reports on the hydrolytic degradation at different pHs as well as toxicity of here investigated materials. Therefore, the main focus was on hydrolysis of star-shaped PCL films in different degradation media through which conditions close to physiological conditions (pH 7.4) and close to the gastric juice (pH 1.0) were imitated. Following the idea to replace the chlorine solvents with the "green" one, we found the ethyl lactate as a perfect candidate for polymer films preparation since this solvent satisfies at least eight of the "Twelve Principles of Green Chemistry."[28] Since our ongoing research is focused on potential application of synthesized star-shaped PCLs as polymer matrix in drug delivery systems, toxicity evaluations were also done. In term of determination of star-shaped PCL cytotoxicity, health human fibroblasts (MRC5) were applied for cell survival assessment, while the zebra fish model, that has not been used for these polymers so far, provided the information about their embryotoxicity.

Experimental part

Materials

ε-Caprolactone (ε-CL, Acros Organics, 99%) was purified with CaH_2 by vacuum distillation. Trimethylolpropane (TMP), ditrimethylolpropane (diTMP), pentaerythritol (PERT), and dipentaerythritol (diPERT) (Fluka) were recrystallized from

hot acetone and then dried under vacuum at room temperature for 24 h. Stannous octoate, $(Sn(Oct)_2,$ 99%) purchased from Aldrich was used as received. Toluene (Aldrich) was dried over molecular sieves (4 Å), methanol (Zorka Pharma, Serbia), chloroform (Carlo Erba), and diethyl lactate (Sigma Aldrich) were used without further purification.

Synthesis of star-shaped PCL polyesters.

Star-shaped PCL polyesters with different number of arms, were synthesized by ring-opening polymerization (ROP) of ε-CL in bulk, initiated by hydroxyl groups of multifunctional alcohols and catalyzed by $Sn(Oct)_2$ as previously reported.[29] The number of arms was dictated by the number of hydroxyl groups of used alcohols: three, four, and six hydroxyl groups (TMP, PERT, diTMP, and diPERT, respectively). The linear PCL homopolymer was synthesized for comparison purpose: control of molecular weight was achieved by using ethanol. Typical polymerization procedure for star-shaped PCL was as follows: the calculated amount of multifunctional core (e.g. 0.340 g pentaerythritol, 2.5 mmol), $Sn(Oct)_2$ $(1 \times 10^{-4}$ mol calculated to 1 mol of monomer, ε-CL) and ε-CL (50.0 g, 2.5 mmol, in the reaction with PERT) were placed in a three-necked flask equipped with condenser under a nitrogen atmosphere. The reaction mixture was heated at 160°C for 24 h under stirring, the resulting product was dissolved in chloroform and precipitated into excess (10 times) of cold methanol. Star-shaped PCL polymers was obtained after filtering and drying in the vacuum oven at room temperature until constant weight was reached.

Preparation of polymer films

Polymer films were prepared from a 6 wt% ethyl lactate solutions by the solvent casting method in glass Petri dishes. Prepared solutions were heated over night at 50°C, due to a low evaporation rate of ethyl lactate. After solvent evaporation, polymer films were dried in vacuum oven. The films were cut into the rectangles (10×10 mm, thickness 200 μm, weight about 30 mg) and used for further experiments.

Polymer characterization

Nuclear magnetic resonance (^{1}H, ^{13}C NMR) spectroscopy.

The chemical structure of the synthesized star-shaped PCL polyesters was confirmed by NMR spectroscopy. All NMR spectra were recorded on Bruker Ascend 400 instrument (^{1}H NMR at 400 MHz, ^{13}C NMR at 100 MHz) using deuterated chloroform ($CDCl_3$) as a solvent and tetramethylsilane (TMS) as an internal standard.

Gel permeation chromatography.

The molecular weights (M_n and M_w) of polyesters were determined by gel permeation chromatography (GPC) analysis. The measurements were performed on a Waters 600E apparatus (RI detection) equipped with a Styragel columns. Poly(styrene) standards were used for calibration and THF as the eluent at a flow rate of 1.0 mL/min at 30°C.

Viscosity measurements.

The viscosity measurements were performed at 25 ± 0.02°C using an Ubbelohde capillary viscometer, in chloroform. The intrinsic viscosity was calculated from these measurements.

Differential scanning calorimetry and thermogravimetric analysis.

Coupled differential scanning calorimetry (DSC)/thermogravimetric (TG) analysis was performed on a TA Instruments SDT Q600 instrument. All the measurements were done in a temperature range of 25°C to 600°C, at the heating rate of 10°C/min, in a nitrogen atmosphere. Weights of samples were about 5 mg.

Wide angle X-ray diffractometry.

In order to evaluate the crystalline structure of linear PCL and star-shaped PCLs, X-ray diffraction was performed on an ItalStructure APD2000 diffractometer in a Bragg-Brentano geometry with CuK-α ($\lambda = 0.15418$ nm) radiation. The polymer samples were scanned from 5° to 40° 2θ with step-time of 0.5 s and step width: 0.02°.

ATR-infrared spectroscopy.

The structure of the synthesized PCL based polyesters was examined by Fourier transform infrared (FTIR)

spectroscopy. The IR spectra were recorded in the range of 400 to 4000 cm^{-1} using an IR-Affinity spectrophotometer (SHIMADZU, Japan). The number of scans was 100, collected in the range of 4000 to 400 cm^{-1} with a spectral resolution of 4 cm^{-1}, at room temperature.

Atomic force microscopy analysis. Different surface morphology, before and after hydrolysis was investigated by atomic force microscopy (AFM). AFM analysis was performed on Nano-Scope III A (Veeco Digital Instruments, USA) device. Nanoscope image processing software was used for image analysis by which surface roughness (route mean square, RMS) was determined from the surface area of 50 × 50 μm^2.

Inductively coupled plasma optical emission spectroscopy, ICP-OES analysis. The concentration of remained Sn coming from the catalyst in the purified polymers was determined using the inductively coupled plasma atomic emission spectroscopy performed on a Thermo Scientific ICAP 6500 Duo ICP system (Thermo Fisher Scientific, Cambridge, United Kingdom). Tin plasma standard solutions Specpure®, Sn 1000 $\mu g/mL$ certified by Alfa Aesar GmbH & Co KG, Germany were used to prepare the calibration solutions for ICP-OES measurements. The quantification of the tin in solutions was measured at the emission wavelength 189.989 nm.

Hydrolytic degradation

In order to assess the influence of pH of degradation medium, but also to imitate conditions close to physiological and gastric juice conditions, hydrolytic degradation was carried out in two different solutions: phosphate buffer solution (PBS, pH 7.4, prepared by dissolving 56.8 g $Na_2HPO_4 \times 2H_2O$ and 36.4 g KH_2PO_4 in 1000 mL of distilled water) and in hydrochloric acid solution (HCl, 0.1 M, pH 1.0). Polymer films were placed in small vials filled with 10 mL of degradation medium. The samples were thermostated at 37°C for 5 weeks and the solutions were changed every week. Two replicates were taken out of the solution at predetermined time intervals, washed with distilled water and vacuum-dried at room temperature up to a constant weight.

The degradation rate was followed by determining the weight loss of the polymer films by comparing dry weight (m_1) at a specific time of film degradation with the initial weight (m_0) according to the equation:

$$weight\ loss\ (\%) = \frac{m_0 - m_1}{m_0} \times 100$$

Sample preparation for cytotoxicity and embryotoxicity test

Polymer powders were aseptically grinded and immersed (10 mg/mL) either in RPMI-1640 (Sigma Aldrich) medium or E(mbryos) water (0.2 g/L of Instant Ocean® Salt in distilled water) for cytotoxicity and embryotoxicity evaluation, respectively. Polymer suspensions were incubated at 37°C for 72 h, shaking at 180 rpm. Then, suspensions were briefly centrifuged and the supernatants (polymer extracts) were used in different concentrations. Finely suspended polymer powder (200 $\mu g/mL$) was also added directly to cells or zebra fish embryos.

In-vitro cytotoxicity. Cytotoxicity (antiproliferative activity) was measured using standard MTT assay[30] and methods suitable for materials testing.[31] MRC5 cells (human lung fibroblast, obtained from ATCC) were treated with 100%, 50%, 25%, and 12.5% (v/v) polymer extract as well as with 200 $\mu g/mL$ of the grinded material and incubated for 48 h. Control cultures were treated only with growth medium and blank wells also contained growth medium (200 μL). Cells proliferation was determined using MTT reduction assay by measuring the absorbance at 540 nm on Tecan Infinite 200 Pro multiplate reader (Tecan Group, Männedorf, Switzerland). The MTT assay was performed in triplicates and the results were presented as percentage of the control (untreated cells) that was arbitrarily set to 100%.

Embryotoxicity. Toxicity assessment of the polymers has been performed in vivo using the zebra fish model during a period of 5 days. Embryos were divided in two experimental groups: the embryos exposed to embryo water (in which the grinded polymers were extracted over 72 h at 37°C and 180 rpm and applied as 100%, 50%, 25%, and 10% solution), and the embryos exposed to the grinded polymer (200 μg/mL).

Evaluation of acute toxicity of the polymers in the zebrafish model was carried out according to general rules of the OECD Guidelines for the Testing of Chemicals (OECD, OECD Guidelines for the Testing of Chemicals, 2013, Test No. 236.). All experiments involving zebrafish were performed in compliance with the European directive 2010/63/EU and the ethical guidelines of the Guide for Care and Use of Laboratory Animals of the Institute of Molecular Genetics and Genetic Engineering, University of Belgrade.

Zebrafish embryos were produced by pairwise mating, collected and distributed into 24-well plates containing 10 embryos per well and 1 mL E water, and raised at 28°C. At 6 h post fertilization (hpf) embryos were exposed to different concentrations of the supernatant (material extract) (10%, 25%, 50%, and 100%, v/v) and the grinded material (200 μg/mL). Embryo water was used as negative control. Experiments were performed three times using 30 embryos per concentration.

Apical endpoints for the toxicity evaluation (Supplemental material Table S1) were recorded at 24, 48, 72, and 96 hpf using an inverted microscope (CKX41; Olympus, Tokyo, Japan). Dead embryos were counted and discarded every 24 h. At 96 hpf, embryos were inspected for heartbeat rate, anesthetized by addition of 0.1% (w/v) tricaine solution (Sigma-Aldrich, St. Louis, MO), photographed and killed by freezing at −20°C for ⩾24 h.

Results and discussion

Synthesis of star-shaped PCLs

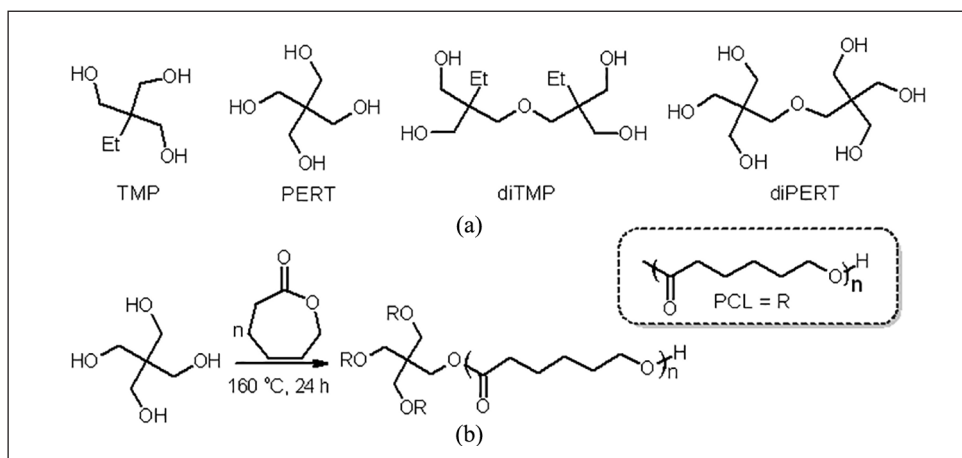For the synthesis of star-shaped PCLs, different multifunctional cores in order to vary a number of arms were used (Scheme 1). Variation in the number of arms was achieved by using alcohols with three, four and six hydroxyl groups, such as TMP, diTMP, PERT, diPERT, respectively. PCL arm's length was fixed (5000 g/mol) and only multifunctional cores were varied in the ROP synthetic route of ε-CL (Scheme 1). Star-shaped PCLs with different number of arms with controlled PCL length were obtained by adjusting the molar ratio of starting reaction mixture (ε-CL/OH—ratio about 44) (Table 1). The yields of the synthesized PCL polyesters were in the range of 94% to 96%.

Characterization of the synthesized star-shaped PCLs

NMR and GPC analysis. The structure of the obtained polyesters, their molecular weights and composition (CL/OH ratio) were determined by NMR analysis. Figure 1 showed the representative ^{1}H NMR and ^{13}C NMR spectra of PERT/PCL from which chemical structure of star-shaped PCL was confirmed. Spectra of all other synthesized polyesters were interpreted in the same manner. The all detected resonance peaks were attributed to PCL. Therefore, peak that appeared at 4.10 ppm is assigned to methylene proton (5) adjacent to the oxygen atom in the PCL units, while signal at 3.65 ppm came from the terminal methylene (–CH_2-OH) (5') from PCL segment indicating that PCL is terminated by hydroxyl groups.[19] The degree of polymerization, molecular weights of PCL branches for star-shaped polyesters were calculated from the ratio between the integrated area of peaks arising from methylene protons next to the oxygen in the PCL repeat units (4.10 ppm) and those coming from the terminal unit (3.65 ppm) according to the equation:

$$M_n^{NMR} = \frac{I_{4.10}}{I_{3.65}} \cdot M_{CL} \cdot Y + M_i$$

where M_{CL} is molecular weight of repeating unit (114 g/mol), Y is number of arms and M_i is the molecular weight of initiating species (TMP, PERT, diTMP, diPERT).

Scheme 1. (a) Different type of cores (three, four, and six arms) and (b) representative synthesis of four-armed PERT/PCL.

Table 1. Molecular weights, polydispersity index, and intrinsic viscosity of star-shaped PCLs.

Polymer	[CL]/[OH][a,b]	Yield, %	M_n,[a] g/mol	M_n,[c] g/mol	M_n,[d] g/mol	M_w,[d] g/mol	PI[d]	[η], dL/g
PCL	237 (132)	88	10,950		55,400	81,770	1.47	0.68
TMP/PCL	52 (44)	95	17,770	5880	43,230	61,820	1.43	0.51
diTMP/PCL	45 (44)	94	20,520	5070	54,670	73,180	1.34	0.55
PERT/PCL	40 (44)	96	18,860	4680	47,320	62,040	1.31	0.50
diPERT/PCL	43 (44)	94	29,360	4850	67,725	90,290	1.33	0.51

[a]Determined by ^{1}H NMR.
[b]In the parenthesis CL/OH ratio of the starting reaction mixture is given.
[c]Molecular weight of the single arm determined by ^{1}H NMR.
[d]Measured by GPC.

According to ^{1}H NMR analysis, conversion of the ε-CL is supposed to be close to 100%, because of the absence of resonance of the monomer $-CH_2$-COO- at the chemical shift of 2.63 ppm.[32] Data obtained from NMR analysis were summarized in Table 1. As could be noticed, the obtained molecular weights and degree of polymerization were in agreement with the targeted one.

Additional proof of the specified star-shaped PCL polyesters' structure was obtained from the ^{13}C NMR spectrum (Figure 1(b) shows representative spectrum of PERT/PCL polyester). Chemical shifts in the ^{13}C NMR spectra of star-shaped PCLs were similar for all samples, and were as follows: 173.5 ppm (C1), 64.1 ppm (C6), 33.9 ppm (C2), 28.4 ppm (C5), 25.2 ppm (C3), and 24.6 ppm (C4). High intensity signals at 64.0 ppm in the spectrum corresponded to C6 atom in the unit located in the middle of PCL arms, whereas small peak at 62.6 ppm (C6') is indicative for C atom in the unit located at the end of the PCL arms. In the spectra of all polymers, peaks coming from the multifunctional alcohols could not be detected. In addition, carbon atom adjacent to the carbonyl group in CL unit (C2') at the end of PCL arms was also detected. The signal of carbon atoms adjacent to cores (C1') appeared as small peak at 173.0 ppm indicating successful reaction of all OH groups.

The results of GPC analysis are listed in Table 1. According to the GPC analysis, it could be concluded that with the increase of number
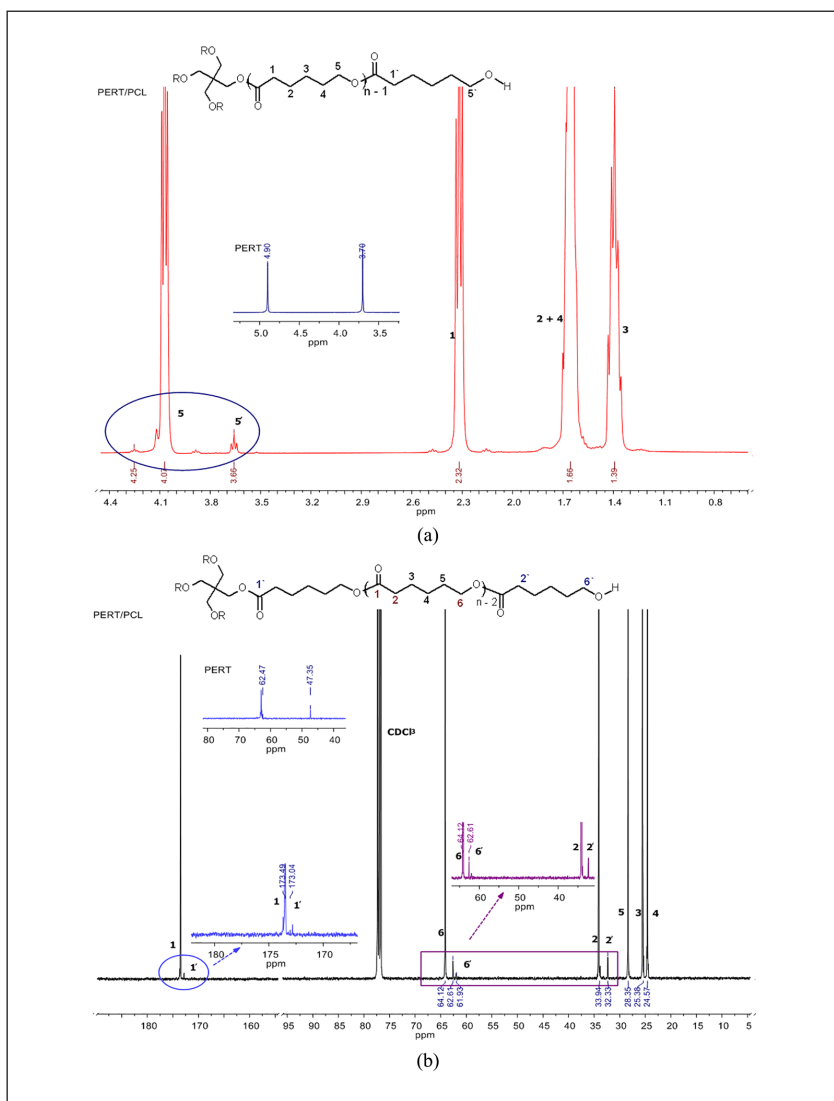
Figure 1. (a) Representative ¹H NMR and (b) ¹³C NMR spectra of PERT/PCL polyester.

of branches, the molecular weights of polyesters increased. The values of M_n of the copolymers determined by GPC were higher in comparison to the M_n obtained by NMR, since the former reflects the hydrodynamic volume of polymer chains in respect to linear polystyrene standards.[33,34] The GPC curves of the synthesized star-shaped PCL polyesters were unimodal with relatively narrow molecular weight distributions. Polydispersity indexes, PI, of

star-shaped polyesters were lower in comparison to linear PCL (1.42), and the increase in the number of branches led to the more narrow distribution. Polyesters with PERT and diPERT as multifunctional core showed the smallest PI values in the whole series (1.23 and 1.25, respectively). The results of viscosity measurements, that is, the intrinsic viscosity values were in agreement with NMR and GPC results and indicated the highest value for linear PCL
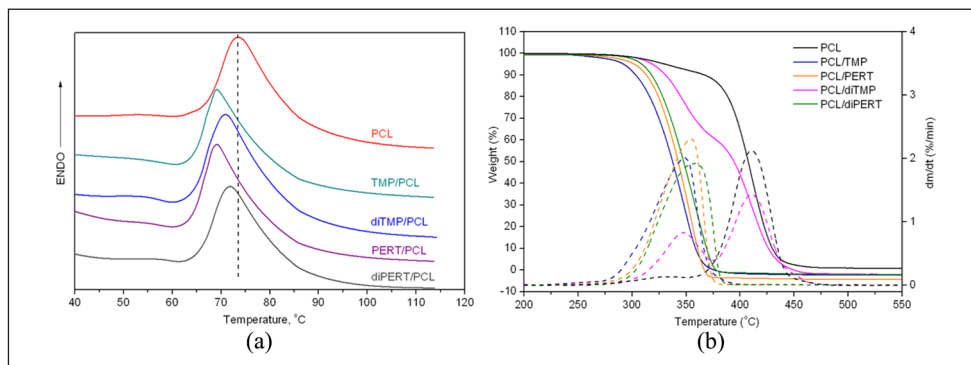
Figure 2. (a) DSC analysis and (b) TG and DTG analysis.

Table 2. DSC and TG analysis results.

Sample	T_m, °C	ΔH_m, J/g	X_c, %	$T_{5\%}$, °C	$T_{50\%}$, °C	$T_{90\%}$, °C	T_{max}, °C
PCL	73.6	58.7	43.1	329.5	406.5	429.7	410.5
TMP/PCL	69.1	57.8	42.5	292.6	337.0	358.4	348.5
diTMP/PCL	71.0	57.0	41.9	319.8	394.8	425.7	346/410.5
PERT/PCL	69.2	61.8	45.4	302.9	343.3	361.2	353.9
diPERT/PCL	72.0	49.0	36.0	309.0	347.6	368.9	357.5

(0.68 dL/g), while the [η] values were similar for all star-shaped polymers. Finally, new PCL based polyesters, with different number of branches and multifunctional cores, with clearly defined structure were successfully synthesized and used for further investigations.

Thermal properties of PCL star-shaped polyesters. The type of multifunctional core and number of arms in star-shaped PCLs significantly affected their thermal properties. Thermal properties of PCL polyesters were characterized using both DSC and TGA. From the DSC melting curves (Figure 2(a)), single, endothermic peak, coming from melting of PCL as only crystalline phase, could be detected for all star-shaped PCL polyesters. The results determined by DSC analysis were presented in Table 2. As was expected, melting temperature of linear PCL was the highest (73.6°C) compared to star-shaped polyesters which T_m values were lower, in the range of 69.1°C to 72.0°C. However, slight decrease in melting temperature could be noticed

with the increase in number of arms but also the influence of molecular weight on T_m values hence the samples diTMP/PCL (four arms) and diPERT/PCL (six arms) possessed higher melting temperatures in comparison to two other star-shaped PCLs due to the higher molecular weight. In contrary to these findings, the obtained melting enthalpy values confirmed the dominant influence of branched architecture on ΔH_m values. Therefore, TMP/PCL, and diTMP/PCL had the melting enthalpies very similar to linear PCL probably due to the similar molecular weights, while the melting enthalpy of PERT/PCL was the highest in the series and the sample diPERT/PCL possessed the lowest ΔH_m value. Such a high ΔH_m value determined for the PERT/PCL could be explained by symmetric and compact structure of PERT core which further provided better lamellar organization and more efficient crystallization of PCL units in star-shaped PERT/PCL polyester. Finally, the most branched star-shaped architecture (six arms) resulted in the smallest melting enthalpy values, detected for

diPERT/PCL (49.0 J/g), confirming that thermal properties could be successfully tuned by polymer architecture and their molecular weights.[35]

According to degree of crystallinity values (calculated from the ratio of ΔH_m and theoretical value of absolutely crystalline PCL homopolymer, $\Delta H_m° = 136.1$ J/g[36]) listed in Table 2, linear PCL had very similar X_c value to TMP/PCL polymer, because of the similar molecular weight. Also, this result referred to the negligible influence of small number of arms on crystallization patterns in the case of similar molecular weight. Further increase in number of arms resulted in decrease in X_c value as was observed for polymer diTMP/PCL. However, the other two star-shaped PCL polymers seem not to fit into observed pattern. In fact, symmetric, compact architecture of PERT core and further symmetric star-shaped PERT/PCL structure allow PCL chains to better organize in well-ordered structure resulting in the highest X_c value in the whole series. Despite the symmetric diPERT structure, branched, flexible structure of diPERT/PCL polyester was responsible for the lowest degree of crystallinity (36.0%). This could be attributed to larger number of free chain ends disrupting well-ordered crystalline structure and further affected crystallization.[37] Summarizing presenting thermal analysis results, it could be inferred that thermal properties of star-shaped polymers based on PCL are both dictated by number of arms, architecture of core, and final molecular weight of polymer.

Thermal degradation of linear PCL has been extensively investigated so far, and some studies proposed that linear PCL degrades trough a single-step unzipping mechanism,[38] while some authors claimed that degradation proceeds as two-step mechanism (parallel or sequential): statistical rupture of polymer chains and unzipping degradation.[39,40] Figure 2(b) depicted the TGA thermograms and DTGA curves of star-shaped polyesters with various arm numbers, in which great difference in thermal stability between samples could be seen. From the all investigated samples, linear PCL showed the best thermal stability, while for the star-shaped PCL polymers characteristic degradation temperatures ($T_{5\%}$, $T_{50\%}$, $T_{90\%}$, and T_{max}) were

shifted toward lower temperature regions. The TGA thermograms depicted one peak at different temperatures, ranged from 348.5°C to 357.5°C for star-shaped PCL polymers, and at 410.5°C for linear PCL. An exception was the sample diTMP/PCL which had two inflection points at 346°C and 410.5°C, respectively indicating two-stage degradation mechanism. The values of characteristic temperatures point to thermal stability of the samples: the higher temperature in the beginning of thermal degradation process means the better thermal stability of star-shaped PCL polyesters. Consequently, three armed sample TMP/PCL reflected the smallest thermal stability, probably because of the smallest molecular weight compared to other samples. With the increase in number of arms, thermal stability was enhanced, because more arms number means higher molecular weight which has a great impact on thermal stability. In contrast, the sample diTMP/PCL degraded in two stages probably because of the dominant effect of branched architecture in comparison to molecular weight. Despite the highest number of arms of diPERT/PCL, the highest molecular weight of this polyester was responsible for better thermal stability compared to other star-shaped PCLs. Since the star-shaped PCLs with more arms possess more end groups which could promote the unzipping mechanism of thermal degradation, it was expected for the polymers with more arms to be less thermally stable. In the comprehensive study which refers to the thermal stability of star-shaped PCLs,[19] where both influence of number of arms and polymer molecular weight were investigated, the authors declare the great influence of both number of arms and polymer molecular weight on thermal degradation properties. However, Xie et al. claimed that degradation of star-shaped PCL polyesters took place through two-stage mechanism, at different temperatures, none of which is depolymerization which starts from the end groups of PCL. They concluded, according to the obtained different degradation products in the first and the second stage, that it was more likely to be random chain cleavage of PCL arm occurring through two
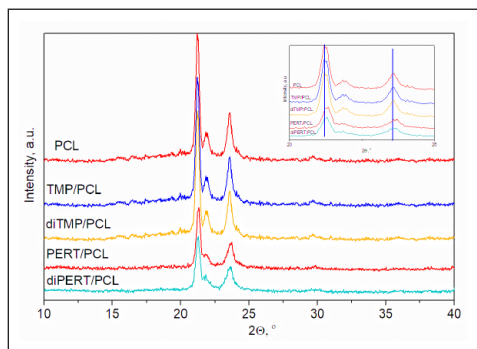
Figure 3. WAXD analysis of linear PCL and star-shaped PCLs polyesters.

different mechanismus.[19] For star-shaped PCLs of lower molecular weight, the mass loss occurred mainly in the first stage (TG curve with single inflection at low temperature), while for higher molecular weights it happens mainly in the second stage (single inflection point at higher temperature). Only for intermediate molecular weights one could clearly observe two inflection points in TG curve, which indicated that mass loss occurred through the both types of thermal degradation processes.[19] Summarizing all previous findings and results presented herein it could be concluded that analyzed star-shaped PCL polymers probably degraded by random chain scission of their arms which occurred by two different mechanisms, while only in the case of the sample diTMP/PCL the both stages could be observed in TG curves. For star-shaped polyesters of lower molecular weight the first mechanism prevails, while for diPERT/PCL of the highest molecular weight among star-shaped PLCs the second mechanism is dominant.

Wide angle X-ray diffractometry. Wide angle X-ray diffractometry (WAXD) analysis was applied to revile the crystalline structure of linear PCL and synthesized star-shaped PCLs and the corresponding diffractograms were presented in Figure 3. As indicated, in the diffractogram of both linear PCL and star-shaped PCLs, three main peaks were observed, two strong, sharp peaks appearing at *2* θ values of

21.2° and 23.6°, while the small intensity peak occurred at *2* θ value of 21.9°. All the star-shaped PCLs crystallize in an orthorhombic crystal lattice with the following parameters: $a = 0.7496$ nm, $b = 0.4974$ nm, $c = 1.7971$ nm, in the same manner as linear counterpart.[41] It was also noticeable that small intensity peak at 22.2° appeared less sharp and broader in the case of PERT/PCL and diPERT/PCL polymers. The WAXD analysis also showed negligible shifting of characteristic diffraction peaks of PERT/PCL and diPERT/PCL polymers to the higher *2* θ values indicating decrease in the dimensions of crystal lattice. The presented data point to the conclusion that the branched architecture did not affect the form of crystal lattice in which PCL crystallize.

Hydrolytic degradation of star-shaped PCLs at different pH values

Gravimetric analysis. Hydrolytic degradation is beneficial for successful application of biopolymers as surgical sutures, drug delivery systems and tissue engineering scaffolds.[42] The degradation behavior of PCL and star-shaped PCLs in the acid medium (pH 1.0) was compared with the one in phosphate buffer solution (PBS) at pH 7.4 to predict their possible degradation behavior in the body, since acid medium imitates conditions close to those in gastric juice and PBS mimics conditions close to physiological conditions. Hydrolytic degradation of semi-crystalline polyesters starts with water diffusion into the amorphous regions, which are less organized and water can easily diffuse, followed by the degradation of crystalline domains that starts when most of the amorphous regions are degraded.[43] Water access is further defined by combined effect of hydrophobicity of the polymers as well as by crystallinity of polymer matrix.[44] Semi-crystalline structure of PCL matrix could restrict water penetration into the polymer bulk which further provided its stability against abiotic hydrolysis.[45] However, the star-shaped architecture of PCL provides lower polymer matrix crystallinity and further improves their biodegradable properties.
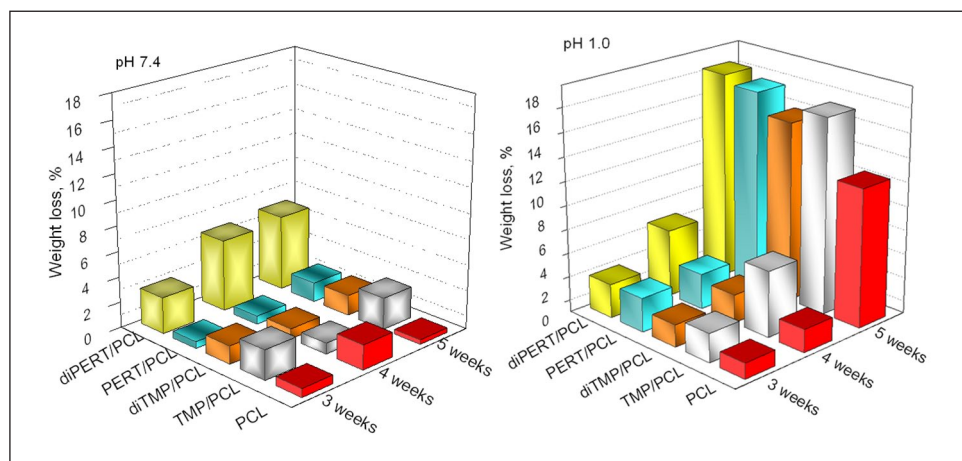
Figure 4. Hydrolytic degradation of PCL and star-shaped PCLs polyesters after 4 and 5 weeks at: (a) pH 7.4 and (b) pH 1.0.

The weight loss of tested star-shaped PCL polymer films as a function of degradation time is presented in Figure 4. After 5 weeks of incubation in PBS, small weight loss for all star-shaped PCLs could be noticed (below 2 wt%), with an exception of the sample diPERT/PCL. Significant weight loss of diPERT/PCL (about 6 wt%, after 5 weeks) was probably due to the most branched structure (six arms) and low degree of crystallinity of this polyester in comparison to the others from the series which allowed water to easily penetrate into a polymer matrix. Also, despite the small weight loss of other samples, TMP/PCL underwent degradation to higher extent (2.5 wt%) which could be explained by the smallest molecular weight in the series of star-shaped PCLs (about 15,000 g/mol). The presented results pointed out that both number of arms, crystallinity and polymer molecular weight dictated hydrolytic degradation rate of the star-shaped PCL polymers. Linear PCL had the smallest weight loss of all investigated samples which points to the difference in degradation ability between linear and star-shaped polymers of the same chemical structure.

The incubation of star-shaped PCL polymer samples in extremely acidic conditions (pH 1.0) resulted in remarkably higher weight loss for all polymer films, after 5 weeks. Results indicated that tested polymer films immersed in hydrochloric acid solution underwent more rapid weight loss compared to those immersed in PBS, indicating the great influence of conditions (pH) on degradation rate and the accelerated hydrolysis when it is catalyzed by acid. While the linear PCL was quite stable against abiotic hydrolysis in PBS, in hydrochloric acid solution significant weight loss (about 10 wt%) was observed. From the other hand side, star-shaped PCLs were more prone to hydrolysis at pH 1.0 resulting in higher weight loss. Also, the trend that the more branched architecture, the higher weight loss, was present, therefore the highest weight loss had the sample diPERT/PCL which actually had the lowest degree of crystallinity. Further, greater degradation ability of PERT/PCL (four arms) and TMP/PCL (three arms) compared to diTMP/PCL could be attributed to the lower molecular weight.

Finally, both number of arms, crystallinity and molecular weight of star-shaped polymers, as well as applied conditions, could be used as a tool in tuning the desirable degradation properties of this type of polyesters, and, in addition, extend their biomedical application.

GPC analysis of degraded polymer films. Degradation of polyesters which contain hydrolysable ester bonds can proceed through two pathways:
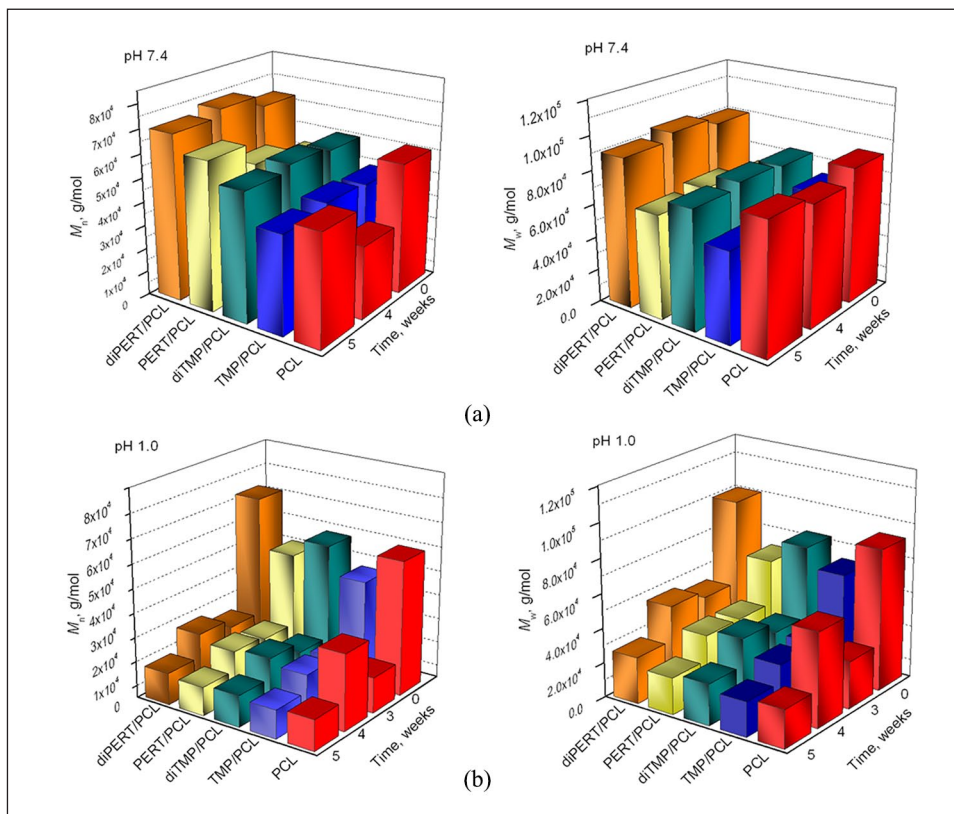
Figure 5. GPC analysis results: (a) M_n and M_w values over 5 weeks of degradation at pH 7.4, (b) M_n and M_w values over 5 weeks of degradation at pH 1.0.

bulk and surface degradation that are stimulated by competition between two processes—water diffusion through the polymer matrix and the hydrolysis of ester bond. Bulk degradation takes place when water molecules penetrate faster through the entire polymer compared to the rate of bond cleavage resulting in random hydrolytic chain scissions throughout the whole matrix in uniform manner. Consequently, oligomers and monomers are formed throughout the matrix, as well as other small molecular weight products (species with hydroxyl and carboxyl end groups). When these products are able to diffuse into the media out of the polymer material, progressive reduction in molecular weight is obtained. In contrast, when these products are not able to diffuse out of the polymer matrix, a concentration gradient of carboxylic acid is formed and the ester bond cleavage

is catalyzed. This phenomenon, known as internal autocatalysis, is manifested in bimodal molecular weight distribution.[42,46] From the other hand side, surface degradation occurs when the water diffusion process is extremely slow compared to the bond cleavage, and the hydrolyzed surface by-products diffuse into the medium before water molecules reach the interior of the polymer matrix. The erosion mechanism is followed by thinning of the material layer by layer from the surface, but molecular weight of the polymer remains intact.

Based on the mechanism of degradation described above, molecular weight analysis can reveal the pathway of degradation. The changes in molecular weight over time, at different pH values were presented in Figure 5. Small changes in molecular weights of polymer films incubated in PBS were in agreement with their
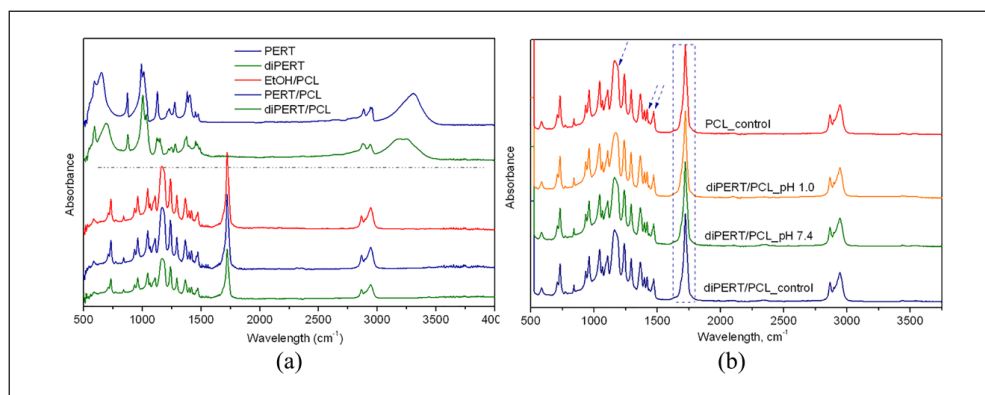
Figure 6. FTIR analysis: (a) representative spectra of star-shaped PCLs and (b) representative spectra of diPERT/PCL after 5 weeks of degradation at pH 7.4 and pH 1.0.

small weight loss and implied that star-shaped PCLs were hydrolytically stable under physiological conditions for up to 5 weeks. Despite the insignificant weight loss of linear PCL, reduction in the M_n (45% after 4 weeks and 15% after 5 weeks) and M_w (10% after 4 weeks and 5% after 5 weeks) values indicated bulk degradation mechanism of hydrolysis. Molecular weight distributions remained almost constant with time.

The acidic environment accelerated the cleavage of ester bonds and led to a greater decrease in molecular weight in a short time. Although insignificant weight loss after 3 weeks of degradation were detected (below 4 wt% for all tested samples), remarkable reduction in M_n and M_w values (70%–80% compared to the starting ones) highlighted random chain scission in the beginning of degradation. Four weeks of immersion in acidic medium resulted in decrease in molecular weight expressed as percentage decrease as followed: 43% for linear PCL, 57% for TMP/PCL, 62% for diTMP/PCL, 59% for PERT/PCL, and 67% for diPERT/PCL. After 5 weeks in acidic medium, there was no greater change in molecular weight in comparison to 3 weeks, while the physical mass continued to decrease. This result may imply that massive loss of degradation products such as oligomers mostly leaked out of the remaining polymer matrix which retained constant value of molecular weight up to 5 weeks of degradation. Also, molecular weight distribution

was broader (ranged from 1.7 to 2.1 in comparison to the starting polymer which PI values were in the range of 1.2 to 1.4) but unimodal peak in chromatogram was detected for all degraded samples which excluded any auto-acceleration in the interior of the polymer sample.

FTIR analysis of degraded samples. Fourier transform infrared spectroscopy was also employed to characterize the structure of star-shaped PCLs and to give more information about their hydrolytic stability. In the recorded spectra (Figure 6(a)), only PCL characteristic peaks were visible; a band characteristic for the ester carbonyl at 1720 cm^{-1}, and two bands for CH$_2$ symmetric and asymmetric stretching at around 2943 cm^{-1} and 2864 cm^{-1}. An absorbance peak at 1294 cm^{-1} coming from the C-C and C-O stretching in the crystalline phase, and the band at 1164 cm^{-1} coming from the C-C and C-O stretching modes in the amorphous phase of PCL were also apparent. Band at 1239 cm^{-1} could be also easily identified and attributed to the asymmetric-COC stretching mode.[23,47] Characteristic hydroxyl group bands from multifunctional cores, visible in the region from 3000 to 3500 cm^{-1}, were not detected in the star-shaped PCLs, confirming the structure of synthesized polyesters and the reaction between –OH functional groups and carbonyl group of CL.

Table 3. Weight loss and crystallinity index from FTIR analysis after 5 weeks at pH 7.4 and pH 1.0.

Sample	Weight loss, %	Crystallinity index[a]
	pH 7.4	
PCL	0.4 ± 0.2	64 (61)
TMP/PCL	2.5 ± 2.6	64 (62)
diTMP/PCL	1.6 ± 0.1	63 (62)
PERT/PCL	1.5 ± 0.5	63 (62)
diPERT/PCL	5.9 ± 3.8	63 (62)
	pH 1.0	
PCL	11.6 ± 1.8	70 (61)
TMP/PCL	16.3 ± 3.4	70 (62)
diTMP/PCL	15.0 ± 3.5	71 (62)
PERT/PCL	16.7 ± 2.3	70 (62)
diPERT/PCL	17.4 ± 2.3	72 (62)

In the parenthesis values for non-degraded samples are given.
[a]Intensity ratio of peaks at 1294 and 1167 cm^{-1}.

After 5 weeks of hydrolysis, both in PBS and hydrochloric acid, all the characteristic peaks inherent to PCL were preserved after degradation and there were no visible changes in spectra. In order to understand the hydrolysis phenomena of star-shaped PCL films, the crystallinity index was calculated from the intensity ratio of characteristic peaks indicated in Figure 6(b).[47] The obtained results were listed in Table 3. After 5 weeks of degradation in acidic medium, values of crystallinity index were considerably higher compared to control ones. The crystallinity index was calculated as the intensity ratio of the peaks at 1294 cm^{-1} (C-C stretching in crystalline region) and at 1167 cm^{-1} (C-O band stretching in amorphous phase of PCL). The increase in crystallinity index values could be taken as an indication that the hydrolysis of the amorphous regions proceeded ahead of the crystalline regions.

Changes in crystallinity index of star-shaped PCL films incubated in PBS were negligible which was in agreement with the small weight loss of those samples and confirmation of stability of star-shaped PCLs against hydrolysis at pH 7.4.

Morphological characterization of polymer films after degradation. The information about the surface morphology of the PCL and star-shaped PCL polymer films before degradation and after 5 weeks of immersion in PBS and HCl solution can be inferred from the 3D AFM images depicted in Figure 7. From the presented micrographs of the native films before degradation, the absence of any regular features such as lamellar structure or spherulites on polymer surface could be noticed. This behavior could be a consequence of different factors affecting a polymer film formation from the solution such as polymer solution viscosity (ethyl lactate polymer solutions had relatively high viscosities since the viscosity of pure ethyl lactate is relatively high (about 2.55×10^{-3}Pa s[48]), slow evaporation rate of non-volatile EL and the affinity of EL systems with glass substrate (the glass surface is hydrophilic and EL is relatively polar solvent).[49,50]

AFM micrographs recorded after 5 weeks of immersion in PBS and HCl revealed significant changes in polymer films morphology after acidic hydrolysis, while polymer films surface stayed almost intact even after 5 weeks in PBS. The PCL and star-shaped PCL polymer films appeared to be smooth before degradation, especially in the case of polymer film from the linear PCL according to the absence of light colored area on micrographs, which indicated higher regions on film surface. In contrast, polymer films degraded at pH 1.0 showed completely different morphology in comparison to non-degraded films and those tested in PBS, and the appearance of lighter regions on photos was more frequent indicating rougher surface as a consequence of polymer film erosion.

Since the AFM analysis highlighted changes in surface of polymer films, surface roughness values, RMS, estimated from AFM photos were calculated in order to quantify the degradation (Figure 8). For the RMS calculation, representative, small areas were chosen (50 μm^2). While the RMS of the polymer films degraded at pH 7.4 remained almost the same (in the case of PCL) or changed insignificantly, remarkable changes for the films immersed in acidic
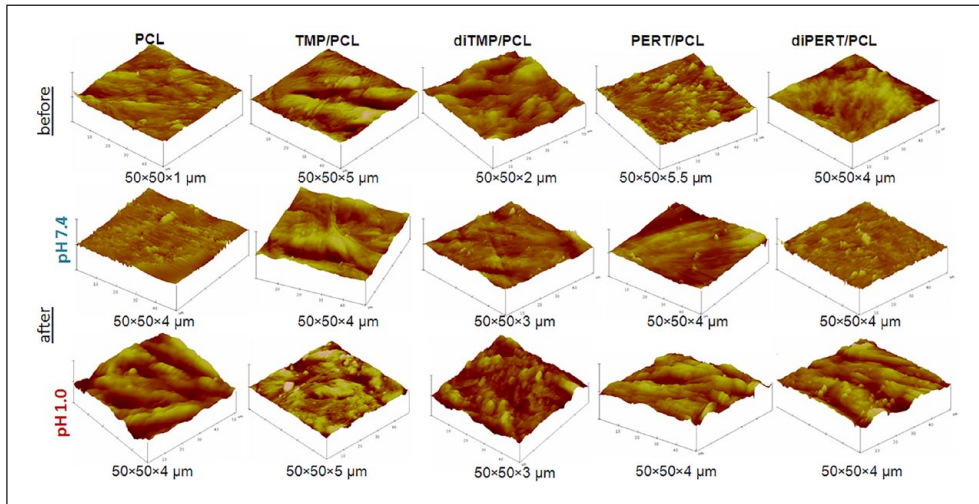
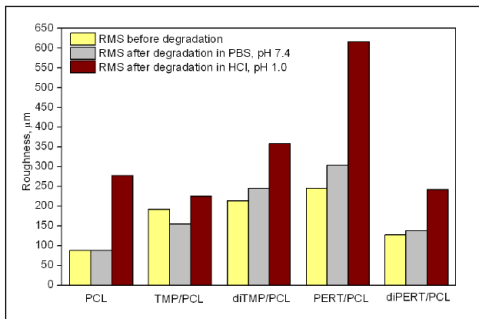**Figure 7.** 3D micrographs of star-shaped PCL polyester films before and after hydrolysis (5 weeks).

Figure 8. Roughness values before and after degradation of PCL and star-shaped PCL polymer films. (Above the bars, weight loss percentage were given).

medium could be noticed. Analyzing the presented RMS values, the RMS value of PERT/PCL polymer film degraded at pH 1.0 appeared as the highest, but actually the starting RMS value, of non-degraded analogue, was the highest in the series of tested polymer films. Expressed in percentage, RMS value of PERT/PCL increase for 251%, while for the linear PCL the increase was approximately 315%. Other samples from the star-shaped PCL series showed the increase in surface roughness as followed: RMS of TMP/PCL samples after degradation increased for 117%, diTMP/PCL for 168%,

while the RMS of diPERT/PCL was higher for 251% in comparison to starting one. Although the correlation between weight loss and changes in RMS values (for example the higher weight loss, the greater increase in RMS) through the series could not be observed, the RMS values of degraded polymer films was used to confirm changes in films surface and to imply the erosion of polymer surface.

Cytotoxicity and embryotoxycity tests

Cytotoxicity tests. A new polymer material that could be potentially applied in biomedicine must undergo nonclinical safety assessment, which includes in-vitro cytotoxicity. Cytotoxicity of linear PCL and star-shaped PCLs was evaluated by standard cell viability assay using normal human fibroblasts (MRC5) exposed to polymer extracts for 48 h. From the presented histogram (Figure 9), it could be seen that polymers' extracts apart from PERT/PCL showed no cytotoxicity in concentrations of 12.5% and 25% with cell survival above 80%. Polymer samples PCL, TMP/PCL, and PERT/PCL showed cell survival between 50% and 40% at 100% concentration of extract, while TMP/PCL showed similar effect even at 50% polymer extract. Also, from the representative photos in Supplemental Figure S1, it was
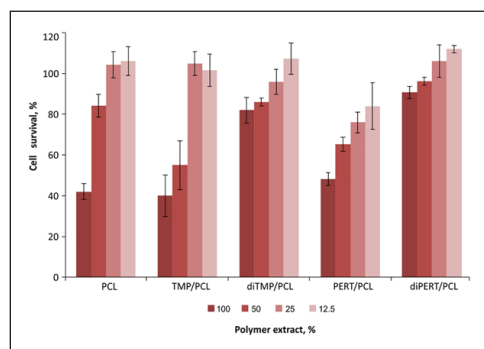
Figure 9. Cytotoxic effects of PCL and star-shaped PCLs extracts of different concentrations.

confirmed that cells appeared with no changes in morphology under the tested conditions. Of all tested materials, extract of diPERT/PCL showed no cytotoxicity under these conditions. Analyzing the highest concentration of applied polymer extract, 100%, it could be noticed that star-shaped polymers with the highest number of arms (diTMP/PCL and diPERT/PCL) appeared as non-toxic with cell survival above 80% suggesting these polymers as the most suitable candidates for biomedical application. The antiproliferative activity of some of the polymer samples might be attributed to the presence of tin residues coming from tin(II)octoate used as catalyst for synthesis. It is relatively difficult to remove tin residues from the synthesized products during the purification step and its toxic effects on cells have been already proved.[51,52] Despite the toxic effects of tin-based catalyst, tin(II)octoate has been approved by FDA (Food and Drug Agency), but most of all, only by using this catalyst high molecular weight polymers required for fabrication can be obtained in comparison to other bio-friendly catalysts. The final concentration of tin found in polymers by ICP-OES analysis was in the range of 94.6 to 134.3 ppm (PCL 97.0 ppm, TMP-PCL 117.6 ppm, diTMP/PCL 134.3 ppm, PERT/PCL 130.1 ppm, and diPERT/PCL 94.6 ppm) which is considerably lower and within the order of magnitude of few previously reported data,[53] but it seemed that the used cell system was sensitive, even to the small concentrations of tin. PCL and PCL based polymers have been recognized as a suitable

substrate for cell growth.[54,55] According to almost the same concentrations of residual catalyst (about 90 ppm) in linear PCL and diPERT/PCL polymer (with the largest number of arms, six), it could be concluded that branched PCL polymers are even more suitable biomaterials for cell adhesion and cell growth compared to their linear counterpart. Given that monomer/catalyst ratio remained constant for the synthesis of all star-shaped PCLs and precipitation of all polymers was carried out in the same manner, metal recoveries is more likely to come from the low solubility of the metal salts, hence tin stayed trapped within the polymer. Some previous reports has shown that tin residues in PCL films intended for biomedical application as high as 3770 ppm showed no cytotoxic effects.[52] The different behavior obtained in this study might be also due to the form in which polymers were used for the tests, that is, powder with high contact area in comparison to the films used in previous studies. The final polymer samples possessed different architecture resulting in possible different interaction of remained tin and polymers which further led to the different cytotoxic effects.

Generally, analyzing the obtained results, we could deduce that, at lower concentration, tested polymers showed no-cytotoxic effects with diPERT/PCL being the least cytotoxic at all used concentrations. These findings suggested the investigated polymer material as promising candidate for biomedical application.

In vivo toxicity evaluation in the zebrafish model. In order to address whether the tested biopolymer materials are safe for the human use, we evaluated their toxicity in the zebrafish (*Danio rerio*) model, which bridges in vitro cell-based models and in vivo mammalian models. In recent years, the zebrafish emerged as an universal biotechnological platform for toxicity and biocompatibility evaluation of novel biomaterials, nanomaterials, and drug carriers owing to high molecular, genetic, physiological and immunological similarity to humans, and good correlation in response to pharmaceuticals and bioactive compounds,[56,57] simplifying thus the path to clinical trials and reducing the failure at later stages of testing.[57,58]
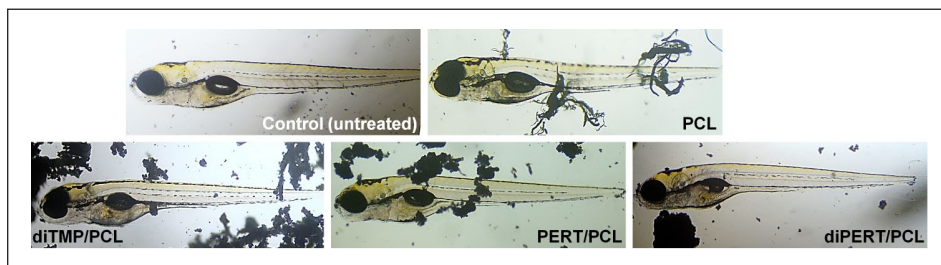
Figure 10. Effects of PCL and star-shaped PCL polymers on zebra fish embryos.

Since the organisms are more sensitive to the chemical insults during embryonic development than as adult, we exposed zebrafish embryos at the 6 hpf stage to the grinded material (200 µg/mL) and embryo water (in which the grinded materials were extracted over 72 h at 37°C and 180 rpm and applied as 100%, 50%, 25%, and 10% suspensions) over a period of 5 days. The obtained results showed that none of the tested materials affected the embryos survival at any experimental group compared to that of the untreated group, neither induced an appearance of teratogenic malformations, the liver necrosis nor disturbed cardiovascular functions (Figure 10 and Supplemental Table S1.) Moreover, no changes in the embryonic skin surface or fins epithelium have been observed, which were in a direct contact with the grinded materials during 5 days. Taken together, data obtained in the zebrafish model, as a whole organism system, indicate biosafety of the tested material, contrary to slight toxicity observed in the cell culture assay.

Conclusion

Well-defined star-shaped PCLs with three, four and six arms of similar length have been successfully designed and synthesized in order to create new material with lower crystallinity compared to linear PCL and to further improve degradability of PCL based polyesters. The degradation process was defined in terms of weight loss, changes in molecular weight and by using FTIR and AFM analysis. Our findings revealed great stability of star-shaped PCLs against hydrolysis under physiological conditions, while the effective

hydrolysis was obtained in hydrochloric acid solution. Also, this study showed that degradation rate of star-shaped PCLs could be controlled by architecture and molecular weight of star-shaped PCL polymers. According to weight loss measurements and GPC analysis, it was deduced that non-catalyzed and acid catalyzed hydrolysis took place as bulk degradation, followed by surface erosion process which was additionally proved by AFM analysis. Increase in crystallinity index calculated by FTIR spectra for all samples degraded in acidic conditions pointed to the preferential degradation of amorphous part of these semi-crystalline polymers. The created star-shaped PCL polymeric material showed no cytotoxycity effects at low concentrations on normal human fibroblast (MRC5). Polymer extracts of higher concentrations showed some level of cytotoxicity. The zebra fish model indicated the absence of embryotoxicity and teratogenicity.

The presented study provided beneficial information about the hydrolytic behavior and cytotoxicity of star-shaped PCLs which have not been investigated so far. Based on these results, star-shaped PCLs are suitable for biomedical application, as drug carriers, and would be further developed in that direction.

Declaration of conflicting interests

Funding

ORCID iDs

Marijana Ponjavic [iD] https://orcid.org/0000-0003-0264-8639

Marija S Nikolic [iD] https://orcid.org/0000-0001-9594-9101

Supplemental material

Supplemental material for this article is available online.

References

1. Iwata T. Biodegradable and bio-based polymers: future prospects of eco-friendly plastics. *Angew Chem Int Edit* 2015; 54(11): 3210–3215.

2. Ren JM, McKenzie TG, Fu Q, et al. Star polymers. *Chem Rev* 2016; 116(12): 6743–6836.

3. Wu W, Wang W and Li J. Star polymers: advances in biomedical applications. *Prog Polym Sci* 2015; 46: 55–85.

4. Cameron DJA and Shaver MP. Aliphatic polyester polymer stars: synthesis, properties and applications in biomedicine and nanotechnology. *Chem Soc Rev* 2011; 40(3): 1761–1776.

5. Khanna K, Varshney S and Kakkar A. Miktoarm star polymers: advances in synthesis, self-assembly, and applications. *Polym Chem* 2010; 1(8): 1171–1185.

6. Bhagabati P, Hazarika D and Katiyar V. Tailor-made ultra-crystalline, high molecular weight poly(ε-caprolactone) films with improved oxygen gas barrier and optical properties: a facile and scalable approach. *Int J Biol Macromol* 2019; 124: 1040–1052.

7. Woodruff MA and Hutmacher DW. The return of a forgotten polymer—polycaprolactone in the 21st century. *Prog Polym Sci (Oxford)* 2010; 35(10): 1217–1256.

8. Griffith M and Venkatraman SS. Polycaprolactone-based biomaterials for tissue engineering and drug delivery: current scenario and challenges AU – Mondal, Debasish. *Int J Polym Mater Pol Biomat* 2016; 65(5): 255–265.

9. Ponjavic M, Nikolic MS, Nikodinovic-Runic J, et al. Degradation behavior of PCL/PEO/PCL and PCL/PEO block copolymers under controlled hydrolytic, enzymatic and composting conditions. *Polym Test* 2017; 57: 67–77.

10. Ponjavic M, Nikolic MS, Jeremic S, et al. Influence of short central PEO segment on hydrolytic and enzymatic degradation of triblock PCL copolymers. *J Polym Environ* 2018; 26: 2346–2359.

11. Wang J-L, Wang L and Dong C-M. Synthesis, crystallization, and morphology of star-shaped poly(ε-caprolactone). *J Polym Sci Pol Chem* 2005; 43(22): 5449–5457.

12. Cui Y, Ma X, Tang X, et al. Synthesis, characterization, and thermal stability of star-shaped poly(ε-caprolactone) with phosphazene core. *Eur Polym J* 2004; 40(2): 299–305.

13. Núñez E and Gedde UW. Single crystal morphology of star-branched polyesters with crystallisable poly(ε-caprolactone) arms. *Polymer* 2005; 46(16): 5992–6000.

14. Wang J-L and Dong C-M. Physical properties, crystallization kinetics, and spherulitic growth of well-defined poly(ε-caprolactone)s with different arms. *Polymer* 2006; 47(9): 3218–3228.

15. Dini F, Barsotti G, Puppi D, et al. Tailored star poly (ε-caprolactone) wet-spun scaffolds for in vivo regeneration of long bone critical size defects. *J Bioact Compat Polym* 2016; 31: 15–30.

16. García-Olaiz GD, Montoya-Villegas KA, Licea-Claverie A, et al. Synthesis and characterization of four- and six-arm star-shaped poly(ε-caprolactone)-b-poly(N-vinylcaprolactam): micellar and core degradation studies. *React Funct Polym* 2015; 88: 16–23.

17. Zhang Y, Zhao Q, Shao H, et al. Synthesis and characterization of star-shaped block copolymer sPCL-b-PEG-GA. *Adv Mater Sci Eng* 2014; 2014: 6.

18. Lang M, Wong RP and Chu C-C. Synthesis and structural analysis of functionalized poly (ϵ-caprolactone)-based three-arm star polymers. *J Polym Sci Pol Chem* 2002; 40: 1127–1141.

19. Choi J, Kim I-K and Kwak S-Y. Synthesis and characterization of a series of star-branched poly(ε-caprolactone)s with the variation in arm numbers and lengths. *Polymer* 2005; 46(23): 9725–9735.

20. Xie W and Gan Z. Thermal degradation of star-shaped poly(ε-caprolactone). *Polym Degrad Stabil* 2009; 94(7): 1040–1046.

21. Nabid MR, Tabatabaei Rezaei SJ, Sedghi R, et al. Self-assembled micelles of well-defined pentaerythritol-centered amphiphilic A4B8 star-block copolymers based on PCL and PEG for hydrophobic drug delivery. *Polymer* 2011; 52(13): 2799–2809.

22. Sailema-Palate GP, Vidaurre A, Campillo-Fernández AJ, et al. A comparative study on poly(ε-caprolactone) film degradation at extreme pH values. *Polym Degrad Stabil* 2016; 130: 118–125.

23. Chang H-M, Prasannan A, Tsai H-C, et al. Ex vivo evaluation of biodegradable poly(ε-caprolactone) films in digestive fluids. *Appl Surf Sci* 2014; 313: 828–833.

24. Li SM, Chen XH, Gross RA, et al. Hydrolytic degradation of PCL/PEO copolymers in alkaline media. *J Mater Sci Mat Med* 2000; 11: 227–233.

25. Petrova S, Kolev I, Miloshev S, et al. Synthesis of amphiphilic [PEO(PCL)2] triarm star-shaped block copolymers: a promising system for in cell delivery. *J Mater Sci Mat Med* 2012; 23: 1225–1234.

26. Xie W, Jiang N and Gan Z. Effects of multi-arm structure on crystallization and biodegradation of star-shaped poly(ε-caprolactone). *Macromol Biosci* 2008; 8(8): 775–784.

27. Cheng J, Ding JX, Wang YC, et al. Synthesis and characterization of star-shaped block copolymer of poly(ε-caprolactone) and poly(ethyl ethylene phosphate) as drug carrier. *Polymer* 2008; 49(22): 4784–4790.

28. Pereira CSM, Silva VMTM and Rodrigues AE. Ethyl lactate as a solvent: properties, applications and production processes – a review. *Green Chem* 2011; 13: 2658–2671.

29. Ponjavic M, Nikolic MS, Jevtic S, et al. Influence of a low content of PEO segment on the thermal, surface and morphological properties of triblock and diblock PCL copolymers. *Macromol Res* 2016; 24(4): 323–335.

30. Hansen MB, Nielsen SE and Berg K. Re-examination and further development of a precise and rapid dye method for measuring cell growth/cell kill. *J Immunol Methods* 1989; 119(2): 203–210.

31. Jaiswal M and Koul V. Assessment of multicomponent hydrogel scaffolds of poly(acrylic acid-2-hydroxy ethyl methacrylate)/gelatin for tissue engineering applications. *J Biomater Appl* 2013; 27(7): 848–861.

32. Turunen MPK, Korhonen H, Tuominen J, et al. Synthesis, characterization and crosslinking of functional star-shaped poly(ε-caprolactone). *Polym Int* 2002; 51(1): 92–100.

33. Wei Z, Liu L, Yu F, et al. Synthesis and characterization of poly(ε-caprolactone)-b-poly(ethylene glycol)-b-poly(ε-caprolactone) triblock copolymers with dibutylmagnesium as catalyst. *J Appl Polym Sci* 2009; 111(1): 429–436.

34. Huang M-H, Li S, Coudane J, et al. Synthesis and characterization of block copolymers of ε-caprolactone and DL-lactide initiated by ethylene glycol or poly(ethylene glycol). *Macromol Chem Phys* 2003; 204(16): 1994–2001.

35. Magnusson H, Malmström E, Hult A, et al. The effect of degree of branching on the rheological and thermal properties of hyperbranched aliphatic polyethers. *Polymer* 2002; 43(7): 301–306.

36. Jiang Y, Mao K, Cai X, et al. Poly(ethyl glycol) assisting water sorption enhancement of poly(ε-caprolactone) blend for drug delivery. *J Appl Polym Sci* 2011; 122(4): 2309–2316.

37. Choi YK, Bae YH and Kim SW. Star-shaped poly(ether−ester) block copolymers: synthesis, characterization, and their physical properties. *Macromolecules* 1998; 31(25): 8766–8774.

38. Aoyagi Y, Yamashita K and Doi Y. Thermal degradation of poly[(R)-3-hydroxybutyrate], poly[ε-caprolactone], and poly[(S)-lactide]. *Polym Degrad Stabil* 2002; 76: 53–59.

39. Persenaire O, Alexandre M, Degée P, et al. Mechanisms and kinetics of thermal degradation of poly(ε-caprolactone). *Biomacromolecules* 2001; 2(1): 288–294.

40. Sivalingam G, Karthik R and Madras G. Kinetics of thermal degradation of poly(ε-caprolactone). *J Analyt Appl Pyrol* 2003; 70(2): 631–647.

41. Bittiger H, Marchessault RH and Niegisch WD. Crystal structure of poly-ε-caprolactone. *Acta Crystal B* 1970; 26(12): 1923–1927.

42. Göpferich A. Mechanisms of polymer degradation and erosion. *Biomaterials* 1996; 17(2): 103–114.

43. Fukushima K, Feijoo JL and Yang M-C. Abiotic degradation of poly(dl-lactide), poly(ε-caprolactone) and their blends. *Polym Degrad Stabil* 2012; 97: 2347–2355.

44. Castilla-Cortázar I, Más-Estellés J, Meseguer-Dueñas JM, et al. Hydrolytic and enzymatic degradation of a poly(ε-caprolactone) network. *Polym Degrad Stabil* 2012; 97(8): 1241–1248.

45. Fukushima K, Feijoo JL and Yang M-C. Comparison of abiotic and biotic degradation of PDLLA, PCL and partially miscible PDLLA/PCL blend. *Eur Polym J* 2013; 49(3): 706–717.

46. Christopher XFL, Monica MS, Swee-Hin T, et al. Dynamics of in vitro polymer degradation of polycaprolactone-based scaffolds: accelerated versus simulated physiological conditions. *Biomed Mater* 2008; 3(3): 034108.

47. He Y and Inoue Y. Novel FTIR method for determining the crystallinity of poly(ε-caprolactone). *Polym Int* 2000; 49(6): 623–626.

48. Wohlfarth C. Viscosity of ethyl lactate. In: Lechner MD (ed.) *Viscosity of pure organic liquids and binary liquid mixtures*. Berlin, Heidelberg: Springer, 2017, pp. 176–176.

49. Causa A, Filippone G, Acierno D, et al. Surface morphology, crystallinity, and hydrophilicity of poly(ε-caprolactone) films prepared via casting of ethyl lactate and ethyl acetate solutions. *Macromol Chem Phys* 2015; 216: 49–58.

50. Poulard C and Damman P. Control of spreading and drying of a polymer solution from Marangoni flows. *EPL-Europhys Let* 2007; 80(6): 64001.

51. Tanzi MC, Verderio P, Lampugnani MG, et al. Cytotoxicity of some catalysts commonly used in the synthesis of copolymers for biomedical use. *J Mater Sci Mat Med* 1994; 5: 393–396.

52. Schappacher M, Le Hellaye M, Bareille R, et al. Comparative in vitro cytotoxicity toward human osteoprogenitor cells of polycaprolactones synthesized from various metallic initiators. *Macromol Biosci* 2010; 10(1): 60–67.

53. Schwach G, Coudane J, Engel R, et al. Influence of polymerization conditions on the hydrolytic degradation of poly(dl-lactide) polymerized in the presence of stannous octoate or zinc-metal. *Biomaterials* 2002; 23(4): 993–1002.

54. Stafiej P, Küng F, Thieme D, et al. Adhesion and metabolic activity of human corneal cells on PCL based nanofiber matrices. *Mater Sci Eng C* 2017; 71: 764–770.

55. Barbarisi M, Marino G, Armenia E, et al. Use of polycaprolactone (PCL) as scaffolds for the regeneration of nerve tissue. *J Biomed Mater Res A* 2015; 103(5): 1755–1760.

56. Lieschke GJ and Currie PD. Animal models of human disease: zebrafish swim into view. *Nat Rev Genet* 2007; 8(5): 353–367.

57. MacRae CA and Peterson RT. Zebrafish as tools for drug discovery. *Nat Rev Drug Discov* 2015; 14(10): 721–731.

58. Barros TP, Alderton WK, Reynolds HM, et al. Zebrafish: an emerging technology for in vivo pharmacological assessment to identify potential safety liabilities in early drug discovery. *Brit J Pharmacol* 2008; 154(7): 1400–1413.